

Pressing the Limits of Rietveld Refinement*

R. A. Young

School of Physics, Georgia Institute of Technology,
Atlanta, GA 30332, U.S.A.

Abstract

Two examples are given, one with X-ray data and one with neutron data, of the determination of structural detail which appear to be at the edge of current possibility for the Rietveld structure-refinement method. In the first example, 2.2 wt% Sb substituted in $\text{Ca}_{10}(\text{PO}_4)_6\text{F}_2$ was located. X-ray powder diffraction data collected with special attention to intensity precision and scale constancy were used. The problem was solved through comparison of intra-sample site-occupancy ratios between Sb-doped and undoped samples. In the second example, high quality, high resolution neutron powder diffraction data were required. The problem was to distinguish between two subtly different models of kaolinite for which the R -weighted-pattern values differed only by 2 or 3 units in the third digit and, particularly, to understand the basis for the consistent programmatic choice of one of the models (P1) over the other. The answer was found in the calculated and 'observed' intensities for $(h+k)$ -odd reflections; although they were very small, less than 1% of the intensities of the main reflections, many of them were distinctly nonzero. Even though these reflections were not separately observable, because of overlap and small size, they nonetheless correlated with one model sufficiently better than the other to produce the consistent choice.

1. Location of 2 wt% Sb in Fluorapatite

(a) The Problem

In this first example, the challenge was to determine the location of the Sb activator in Sb-doped fluorapatite of the general type which has served as the principal commercial phosphor in fluorescent lighting for the past 40 years. This problem has not been solved before because single crystals could not be prepared with enough Sb to allow its location to be determined by direct-sensing means, e.g. diffraction. Since it is possible to get more Sb into fluorapatite $\text{Ca}_5(\text{PO}_4)_3\text{F}$ in powdered (e.g. polycrystalline) form, the Rietveld structure-refinement (RR) method seems to be desirable—if enough precision can be maintained. X-rays were the clear choice over neutrons in this case because of the higher contrast occasioned by the relatively high Z (=51) of Sb.

* Paper presented at the International Symposium on X-ray Powder Diffractometry, held at Fremantle, Australia, 20-23 August 1987.

(b) Materials and Methods

Preliminary calculations of the powder diffraction patterns to be expected with 1 wt% Sb substituting in each of several plausible modes showed differences of, at most, a few per cent are produced in some of the reflection intensities. Thus, specimens as heavily laden as possible with Sb in a single site and particularly precise X-ray powder diffraction intensity data are required.

Doped fluorapatite powders containing 2.2 wt% Sb were specially prepared in a high-temperature solid-state reaction. [These powders were characterised by B. G. DeBoer of the GTE Lighting Products Division. Details on that and other aspects of this project have been given by DeBoer *et al.* (1988).] It was shown with infrared spectroscopy that the Sb is essentially all in the same site as that occupied by the much lesser amounts of Sb which activate the commercial phosphors.

Digitised X-ray powder diffraction data were collected both with X-rays from a standard sealed-off tube source and from a synchrotron source (NSLS). Each of the two sets of tube data used in the final parts of the work is the sum of two 18 hour runs made without disturbing the sample. The two runs were started at different times of day in order to minimise the effects of long-term, seemingly diurnal, intensity variations at the 1% level. A θ - 2θ diffractometer with a diffracted beam monochromator was used to collect step-scan data from 15° to 130° (2θ) with Cu K α radiation. Because there is essentially no specimen broadening of the reflection profiles of this high-fired material, the step size was made rather small, 0.020° (2θ). The fixed time per step was 20 s. The synchrotron data were collected at beamline X-14 with 15 keV radiation and a step size of 0.0025° (2θ).

The Rietveld refinements (RRs) of the pure and doped fluorapatite structures were carried out in space group $P6_3/m$ with the computer program DBW3.2S(8702), which is an upgraded version of the program described by Wiles and Young (1981) and which can handle with correct statistical weighting both synchrotron X-ray data (varying incident beam intensity, dark current and dead-time corrections) and (separately) multiple-counter neutron data.

The three substitutional models that had been proposed, and therefore were to be tested, were Sb substitution for Ca(1), for Ca(2), or for the phosphorus in the phosphate ion (see Fig. 1), or some combination of these (see DeBoer *et al.* 1988 for further discussion of the origins and rationality of these models). Sb substituted in any of these sites could be expected to reveal its presence by its effect on the refined site occupancy factor of the affected site in a model of fluorapatite in which Sb is not explicitly included. The starting model was that reported by Sudarsanan *et al.* (1972) for a single-crystal synthetic fluorapatite. The thermal parameters were kept fixed at the values reported there, while the positional and site occupancy parameters were refined. The site occupancies for the phosphate oxygens were constrained to vary together (earlier RRs with each varying independently showed no pattern and there was no physico-chemical reason to expect them not to be stoichiometrically related). In order that the overall scale factor could be varied, it was necessary to fix one site occupancy; that of phosphorus was chosen. The atomic scattering factors used were taken from the International Tables for Crystallography, including anomalous dispersion corrections. In the sample material containing the Sb-doped fluorapatite, a small amount of calcium meta-antimonate, used as the source of Sb in sample preparation, was also present. It was included in the RRs as a second phase

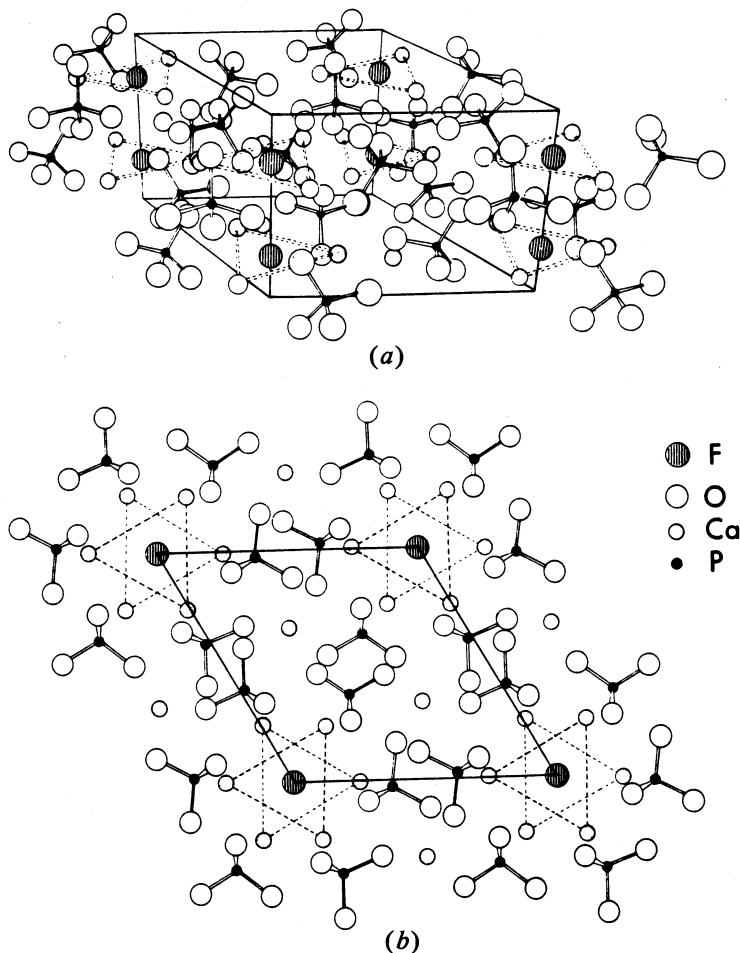


Fig. 1. Fluorapatite showing (a) a perspective view and (b) the view along the direction c . The Ca(2) ions are those shown joined by dashed lines forming triangles; the others, at $\frac{1}{3}, \frac{2}{3}, z$ and $\frac{2}{3}, \frac{1}{3}, z$, are the Ca(1) ions.

(space group $P\bar{3}1m$) with structural parameters fixed at the values determined in a recently completed set of RRs of the structures of calcium, strontium, and barium meta-antimonates (Young *et al.* 1988).

(c) Results

The RRs proceeded well, particularly for the pure fluorapatite, and the positional parameters were all in reasonable agreement with those of Sudarsanan *et al.* (1972). The cell volume was increased by 0.2% by the substitution of the Sb in this doped fluorapatite. Fig. 2 shows one example of observed and refined powder diffraction patterns for the sample material consisting of Sb-doped fluorapatite, plus a small amount of calcium meta-antimonate.

The parameters of direct interest, for this work, are the site occupancies. Those obtained in final, or near final, RRs with one set of data for each specimen material are shown in Table 1 as examples. The site occupancies did not refine to stoichiometric

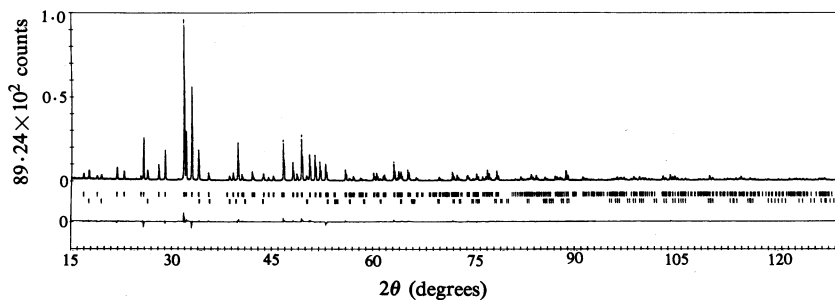


Fig. 2. RR plot for the 2.2 wt% Sb-doped fluorapatite. The observed powder diffraction pattern is shown in the upper field by points plotted with vertical error bars. The calculated pattern based on the final refined model is shown in the same field by the solid curve. The difference, observed less calculated, is shown in the lower field. The positions of the possible Bragg reflections are shown by the short vertical bars in the middle field. There is a separate set of such bars for each of the phases refined simultaneously, Sb-doped fluorapatite and calcium meta-antimonate.

Table 1. Examples of RR results for fluorapatites

Lattice parameters (Å) for the two fluorapatite samples are: pure, R1013F, $a = 9.3692(1)$ and $c = 6.8840(1)$; doped, R1016M, $a = 9.3750(1)$ and $c = 6.8904(1)$

Atom	R file	Fluorapatite specimen	x	y	z	N^A
O(1)	R1013F	Pure	0.3268(5)	0.4861(5)	1/4	0.524(3)
	R1016M	Doped	0.3259(5)	0.4849(5)	1/4	0.520(4)
O(2)	R1013F	Pure	0.5885(5)	0.4670(5)	1/4	0.524(3)
	R1016M	Doped	0.5876(5)	0.4651(6)	1/4	0.520(4)
O(3)	R1013F	Pure	0.3416(4)	0.2573(4)	0.0699(4)	1.048(3)
	R1016M	Doped	0.3437(4)	0.2566(4)	0.0677(5)	1.041(4)
P	R1013F	Pure	0.3980(2)	0.3684(2)	1/4	0.5000
	R1016M	Doped	0.3996(3)	0.3697(2)	1/4	0.5000
Ca(1)	R1013F	Pure	1/3	2/3	0.0011(3)	0.346(1)
	R1016M	Doped	1/3	2/3	0.0015(4)	0.342(2)
Ca(2)	R1013F	Pure	0.2417(2)	-0.0073(2)	1/4	0.517(2)
	R1016M	Doped	0.2397(2)	-0.0064(2)	1/4	0.532(2)
F	R1013F	Pure	0	0	1/4	0.161(2)
	R1016M	Doped	0	0	1/4	0.169(2)

^A Site occupancy divided by the site multiplicity.

values even for the pure fluorapatite. In view of the fact that neither the atomic scattering factors nor the fixed thermal parameters could be expected to be exactly correct for these particular atoms in their particular surroundings, this is not surprising. One can expect, however, that those factors should be identical, or nearly so, for a given atom in both the doped and the undoped fluorapatite. Therefore, intra-sample ratios of refined site occupancies should be much more reliably comparable between samples than are the occupancies alone.

Table 2 shows an array of such ratios obtained from various RRs with various data sets at various stages of refinement. The numbers in the input files (R files) designate the data set. SP in the R file designates synchrotron X-ray data, while M means that

Table 2. RR site occupancy ratios in Sb-doped and undoped fluorapatite

R file ^A	Site occupancy ratios ^B				R_{wp}	R_i
	Ca(2)/Ca(1)	F/Ca(1)	Ca(1)/P	O/P		
<i>Undoped</i>						
RSP21B	0.983	1.040	1.030	1.067	19.6	5.6
RSP21C	0.977	1.029	1.038	1.071	21.9	6.1
RSP21D	0.983	1.043	1.030	1.067	18.9	5.3
RSP21D	0.982	1.044	1.027	1.063	19.6	5.5
R1014F1	0.994	0.973	1.039	1.045	12.6	1.36
R1013F	0.997	0.978	1.037	1.047	12.6	1.35
R1013F	0.996	0.977	1.037	1.048	12.3	1.34
<i>Sb doped</i>						
RSP22B ^C	1.037	0.921	1.021	1.048	30.7	6.7
RSP22MA	1.041	0.924	1.008	1.041	24.2	5.3
RSP22MB	1.039	0.934 ^D	1.025	1.057	60.0	13.1
RSP22MC	1.041	0.917	1.021	1.051	16.0	5.2
R1016M	1.038	0.942	1.027	1.041	13.5	1.44
R1016M	1.037	0.943	1.025	1.041	12.9	1.38
R1015M	1.034	0.922	1.020	1.027	12.9	1.38

^A Wavelength is ~ 0.8279 Å for synchrotron (SP) data and 1.54 Å for other.

^B The e.s.d. in the occupancy ratios, based on the individual site occupancies calculated and reported to four decimal places in the refinement, are 1.2–1.5% with the R1013F and 1014F results, 1.4–1.7% with R1015M and 1016M, 1.0–1.4% with RSP21D, and 1.2–2.0% with RSP22MC.

^C Meta-antimonate phase not modelled.

^D Site occupancies not fully refined.

the meta-antimonate phase was included in the RR. Two R files with the same label are not identical, but were used on different dates. Usually one picked up where the previous refinement (incomplete) had left off. The various 'R values' used here and in Tables 2 and 4 are defined as follows:

$$R_{wp} = \left(\frac{\sum_i w_i \{y_i(o) - y_i(c)\}^2}{\sum_i w_i \{y_i(o)\}^2} \right)^{\frac{1}{2}},$$

where w_i is a weight based on counting statistics and $y_i(o)$ and $y_i(c)$ are the observed and calculated intensities respectively at the i th step in the pattern, and

$$R_B = \frac{\sum_H \{I_H('o') - I_H(c)\}}{\sum_H I_H('o')},$$

where H stands for h, k, l and 'o' is in quotation marks because it is deduced rather than observed directly (Rietveld 1969; Wiles and Young 1981). Further, R_i is the ratio of the obtained value of R_{wp} to that expected on the basis of counting statistics; this quantity is often called 'goodness of fit'.

The first thing to note in Table 2 is the remarkable stability of the results under different starting conditions, different degrees of approach to completion, and different data sets on different specimens of the same sample material. As the values in Table 2 make clear, the actual reproducibility (for a given specimen material and diffraction instrument) in these occupancy ratios is notably better than the e.s.d. for any single ratio value would suggest (see note B in Table 2). Even RSP22MB, for

which $R_{wp} = 60\%$, gave results in line with the others. It is also notable that the synchrotron data lead to results similar to those obtained with the tube data, particularly as far as the inter-sample comparisons are concerned.

The relative constancy of the Ca(1)/P site occupancy ratio between samples suggests that the Sb is not in either site. The alternative is that it occurs in the same proportion in each site in the Sb-doped material. [Since the same ratio was also found in a second differently Sb-doped fluorapatite material actually studied in parallel with the two materials being discussed here (DeBoer *et al.* 1988), this possibility seems quite remote.] The relative constancy of the O/P ratio suggests that there is no significant substitution of SbO_4 for PO_4 . One concludes, therefore, that the Sb is not in either the Ca(1) or the P site.

The Ca(2)/Ca(1) occupancy ratio, on the other hand, is decidedly higher in the Sb-doped material, whether judged from the tube-data or synchrotron-data results. By extension, since the Ca(1)/P ratio is essentially constant between samples, the Ca(2)/P ratio is also decidedly higher in the Sb-doped material.

In Table 2 it is also noted that the F/Ca(1) occupancy ratio is lower in the Sb-doped material. The reason for this has not been determined. Possibly, it may indicate that the substitution of Sb for Ca(2) causes neighbouring F atoms to move away from their special $(0, 0, \frac{1}{4})$ position in pure fluorapatite.

(d) Conclusion about the Sb Location

In view of the consistency of these inter-sample comparisons of intra-sample ratios of refined site occupancies, it was clear that the parameters needed for the determination of the Sb location are stable and not sensitive to the remaining misfits in the RRs which kept the R values high. It was therefore concluded that the Sb substitutes at the Ca(2) site and not at either the Ca(1) or P sites. The effort to locate 2 wt% Sb in fluorapatite with powder diffraction data and the Rietveld method was successful.

2. A Subtle Detail in Kaolinite

(a) The Problem

In this second example of pressing the limits of RR, the challenge was to make a definitive determination of whether the two inner-hydroxyl ions in kaolinite, $Al_2Si_2O_5(OH)_4$, are oriented the same way and, hence, whether the cell is C-face centred or actually primitive ($P1$, $Z = 2$). The differences are known to be subtle, probably at the edge of detectability with the standard deviations in previously reported results. If the two inner-hydroxyl ions are shown to be oriented differently, this would constitute the principal difference between the 'kaolinite' layer in kaolinite and that in the very closely related clay dickite. Dickite does have the different space group Cc and some small differences in physical properties.

The present paper is concerned with the reliability of the determination of this detailed structural feature and, particularly, understanding why a clear choice can finally be made between two different structural results for which the R values (weighted pattern) differ only by 2 or 3 units in the third digit. This paper thus complements a longer study in which the reliability is accepted with less discussion and the emphasis is on the improved structural model obtained with verification that the space group is $P1$ (Young and Hewat 1988).

(b) Kaolinite Structure and Controversy

Kaolin clays have extensive commercial uses, in part because of their layered structures. One of the most extensive uses is for coating essentially all writing and printing paper, except news print, in order to maintain sharp definition of the characters. Fig. 3 shows the structure of the kaolinite layer. Except for the hydrogen atoms in the hydroxyl ions it consists, successively, of a plane of oxygen atoms, a plane of silicon atoms, another plane of oxygen atoms of which one-third (two per cell) are in hydroxyl ions (the 'inner-hydroxyl ions'), a plane of aluminium atoms, and finally a plane of oxygen atoms to all of which are bonded hydrogen atoms to form the 'inner surface' hydroxyl ions which, then, form hydrogen bonds to the next layer. The structure may also be viewed as a 'tetrahedral sheet' (SiO_4 tetrahedra) and an octahedral sheet (oxygen and hydroxyl ions octahedrally coordinating the aluminium ions). The unit cell parameters are $a = 5.149 \text{ \AA}$, $b = 8.934 \text{ \AA}$, $c = 7.384 \text{ \AA}$, $\alpha = 91.93^\circ$, $\beta = 105.04^\circ$ and $\gamma = 89.79^\circ$.

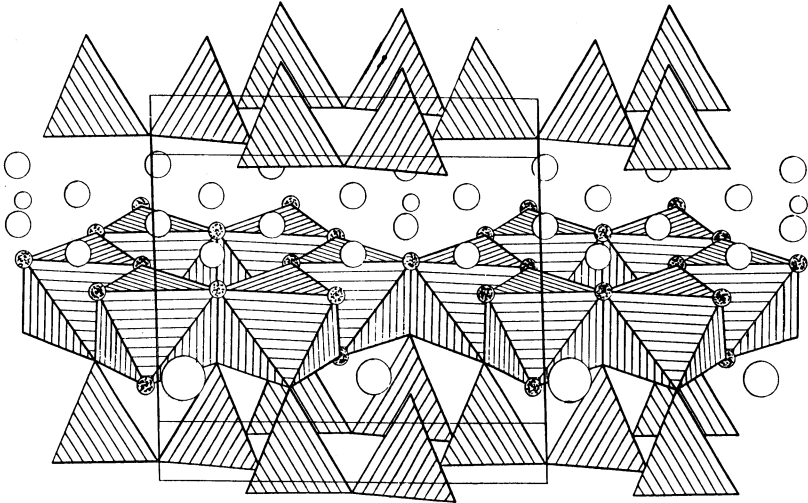


Fig. 3. Final structural model of kaolinite, $\text{Al}_2\text{Si}_2\text{O}_5(\text{OH})_4$ ($Z = 2$), as refined by Young and Hewat (1988). The open circles represent hydrogen atoms. The stippled circles represent OH^- and O^{2-} ions coordinating aluminium atoms. The SiO_4 tetrahedra and the $\text{Al}(\text{O}, \text{OH})$ octahedra are indicated simply as geometric objects. The inner-hydroxyl hydrogen atoms are the ones shown lowest in the figure. Note the different orientations of the two inner-hydroxyl ions. [From Young and Hewat (1988).]

In the most detailed previous work, Suitch and Young (1983; hereafter SY) reported that the cell is primitive, $P1$. However, the departure found from C centring was slight. With rare exceptions (e.g. H2 and H6) all of the atoms except the two inner-hydroxyl hydrogens could be assigned within experimental error to two equivalent groups related by C centring. Only the reported 0.100(16) difference in the z coordinates of the two inner-hydroxyl hydrogens keep them out of this grouping and have the inner-hydroxyl ions differently oriented, one pointing toward a hole in the octahedral sheet and one toward the unoccupied centre of an oxygen triangle formed of the two apical oxygens and the shared basal oxygen of two adjacent SiO_4 tetrahedra.

Adams (1983) however reported from a neutron diffraction study that the two inner-hydroxyl ions are similarly oriented and that the cell is C centred. The SY result has been further questioned by Thompson (1984) and Thompson and Withers (1987). Thus, a definitive resolution of the questions raised seemed necessary. The problem reduces to a convincing determination of the equivalence or inequivalence of the z positions of two hydrogen atoms, possibly the y coordinates of two others and, perhaps, improving the precision of the determinations so that other departures, if any, from C centring might be detected.

(c) Materials and Methods

It was also desired that all 99 atom positional parameters be refined simultaneously in order to avoid the somewhat awkward procedure of using X-ray data for the non-H atoms and neutron data only for the H and O(H) atoms. There seems to be no practical possibility to deuterate the kaolinite to a significant degree non-destructively. Thus, neutron data are required and the high background from the eight H atoms has to be endured. Clearly, the neutron powder diffraction data need to be of high quality and high resolution in order to permit the meaningful simultaneous refinement of 116 parameters (17 non-positional) and the determination of the crucial difference, or lack of difference, in the two inner-hydroxyl hydrogen atom z parameters, which turn out to be about $0.090(7)c$. Two sets of neutron powder diffraction data, for the Young and Hewat (1988) work, were collected with instrument D1A at the Institut Laue-Langevin (ILL), Grenoble, on samples of the essentially faulting-free Keokuk kaolinite.

Table 3. Starting coordinates for the inner-hydroxyl hydrogen in the split centring-imposed model

Atom	x	y	z
H1A	0.253	0.038	0.362
H1B	0.223	0.063	0.269
H5A	0.723	0.563	0.269
H5B	0.753	0.538	0.362

Since verification of a difference in the z parameters of the two inner-hydroxyl hydrogen (iH) atoms would be sufficient in itself to show the absence of C centring, the following stringent test of the accuracy of the SY result was undertaken. Each iH was replaced by two half-atoms with the same x, y parameters but with the two different z parameters reported by SY (Table 3). Since this put one half-iH above and one below the plane containing the attached O(H) atoms ($z = 0.32$), these positions and accompanying orientations of the O(H)-iH vector are readily visualised as 'up' and 'down'. Atom iH(1) up and iH(5) down were then designated as set A. All positional parameters of all atoms were then constrained to a C-centring relationship both initially and during refinement of those parameters and the site occupancies of the iH. Thus, for example, the positions of iH(1)A and iH(5)B were constrained to be C related. The iH site occupancies, the only ones refined, were not. They were constrained so that the total occupancy of the iH(1) sites, and similarly the iH(5) sites, remained at 1.00.

(d) Results

Repeated trial refinements with two independent sets of data (PKAOLIN and PKA086) with two different RR programs on two different computers (Hewat 1973 on the ILL VAX 8600 and DBW3.2S on the GIT CDC-Cyber 855) showed that one of the iH sets always refined away. The set which refined away could be selected by choosing those starting site occupancies to be slightly less than 0.5. If the initial site occupancies were set at precisely 0.500, whether it was the A or B set which survived seemed to be a matter of chance related, one infers, to very minor random differences in the data sets or operations. In terms of crystallography, the two results are equivalent since the two half-cells are constrained to be identical except for the survival of the up-down versus down-up pair; the up-down is transformed to down-up by a $\frac{1}{2}(a+b)$ shift of the origin. Such a shift in this structure is without crystallographic consequence.

Table 4. Tests of possible inner-hydroxyl mutual orientations

RR	Site occupancy				Symbol ^A	R_{wp}	R_i	R_B
	H1A	H1B	H5A	H5B				
CR	1	0	0	1	UU	2.34	2.34	
CQ	0	1	1	0	DD	2.35	2.36	
CP	0	1	0	1	DU	2.25	2.26	6.58
CM	1	0	1	0	UD	2.26	2.26	6.52
CS	0.03(13)	0.97(13)	-0.06(15)	1.06(15)		2.25	2.26	6.48
CN	1.18(13)	-0.18(13)	1.09(12)	-0.09(12)		2.25	2.26	6.53
CL	0.5	0.5	0.5	0.5		2.28	2.29	6.52
SI	1	0	1	0	UD	2.03	2.03	4.90

^A Up (U) and down (D) for the z component of the O-H vector.

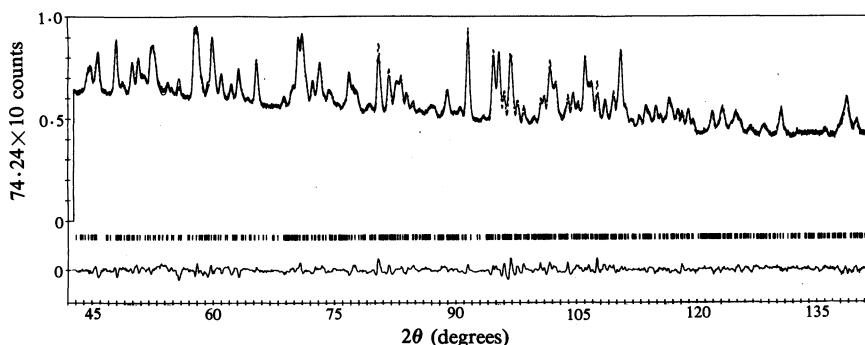


Fig. 4. Section of the Rietveld plot from RR CP provided as an example of the kind of fitting obtained with C centring imposed on all but the site occupancies of the split iH atoms (see Table 4). The plot conventions are as for Fig. 2.

Although the e.s.d. on the refined site occupancies indicate a significant preference for the lack of C-centring of the iH (Table 4), the R values are not lowered much by the simple refining away of the A or the B set. Further RRs were therefore undertaken to show what effects on R values should be expected as a result of differences in the possible combinations of fixed iH occupancies. The principal results are summarised in Table 4, while Fig. 4 shows a section of the Rietveld plot. It is quite clear from the R

Table 5. Calculated and 'observed' Bragg intensities from RR CP

<i>Table 5a. First 60 reflections</i>								
No.	Code	<i>h</i>	<i>k</i>	<i>l</i>	HW	Position	I_{calc}	I_{obs}
1	1	1	0	2	.416	43.182	11.	4.
2	1	2	0	-1	.416	43.740	173.	163.
3	1	1	-3	0	.416	43.811	189.	180.
4	1	1	3	0	.416	44.025	566.	527.
5	1	1	3	-1	.416	44.302	691.	626.
6	1	1	-1	2	.417	44.716	77.	84.
7	1	1	-3	-1	.417	45.038	686.	649.
8	1	2	0	0	.417	45.174	891.	765.
9	1	1	1	2	.417	45.413	225.	186.
10	1	2	1	-1	.417	45.518	0.	0.
11	1	2	-1	-1	.417	45.690	0.	0.
12	1	1	0	-3	.417	46.901	10.	7.
13	1	2	-1	0	.417	46.926	1.	1.
14	1	2	1	0	.417	47.062	2.	2.
15	1	0	0	3	.417	47.401	2073.	1972.
16	1	2	0	-2	.418	48.071	160.	191.
17	1	1	1	-3	.418	48.260	11.	13.
18	1	1	-3	1	.418	48.332	206.	244.
19	1	0	3	-2	.418	48.540	4.	5.
20	1	0	1	-3	.418	48.716	13.	13.
21	1	1	-1	-3	.418	49.080	67.	66.
22	1	1	3	1	.418	49.413	1194.	1192.
23	1	2	1	-2	.418	49.583	2.	2.
24	1	0	1	3	.418	49.596	12.	13.
25	1	1	-2	2	.418	49.738	9.	11.
26	1	2	-1	-2	.418	50.034	2.	2.
27	1	1	3	-2	.418	50.172	1364.	1409.
28	1	0	3	2	.418	50.293	5.	6.
29	1	0	4	0	.419	50.658	408.	456.
30	1	2	2	-1	.419	50.719	71.	79.
31	1	1	2	2	.419	51.020	10.	10.
32	1	2	-2	-1	.419	51.036	548.	563.
33	1	1	-3	-2	.419	51.696	1476.	1449.
34	1	2	0	1	.419	52.004	1130.	1145.
35	1	2	-2	0	.419	52.036	60.	61.
36	1	2	2	0	.419	52.287	815.	896.
37	1	0	4	-1	.419	52.714	217.	332.
38	1	1	2	-3	.419	52.951	8.	18.
39	1	0	2	-3	.420	53.347	54.	125.
40	1	2	-1	1	.420	53.450	4.	9.
41	1	0	4	1	.420	53.822	519.	603.
42	1	2	1	1	.420	53.848	5.	6.
43	1	2	2	-2	.420	54.358	225.	243.
44	1	1	-2	-3	.420	54.480	9.	10.
45	1	0	2	3	.420	54.990	242.	150.
46	1	2	-2	-2	.420	55.202	647.	401.
47	1	1	-4	0	.421	55.811	0.	0.
48	1	1	4	0	.421	56.051	0.	0.
49	1	1	4	-1	.421	56.150	0.	0.
50	1	1	-4	-1	.421	56.976	0.	0.
51	1	2	0	-3	.421	57.171	2436.	2381.
52	1	1	-3	2	.421	57.575	2226.	2235.
53	1	2	-2	1	.422	58.015	620.	531.
54	1	2	1	-3	.422	58.386	4.	3.
55	1	1	0	3	.422	58.471	11.	8.
56	1	2	3	-1	.422	58.681	0.	0.
57	1	2	2	1	.422	58.769	569.	424.
58	1	2	-1	-3	.422	59.049	5.	5.
59	1	2	-3	-1	.422	59.111	0.	0.
60	1	1	3	2	.422	59.312	2200.	2201.

Table 5b. Last 36 reflections

No.	Code	<i>h</i>	<i>-k</i>	<i>l</i>	HW	Position	<i>I</i> _{calc}	<i>I</i> _{obs}
661	1	4	1	-6	.722	147.614	10.	23.
662	1	1	-4	6	.722	147.617	13.	30.
663	1	2	3	-7	.729	148.007	15.	29.
664	1	5	2	-3	.733	148.277	0.	0.
665	1	2	-7	3	.737	148.518	11.	10.
666	1	0	9	0	.738	148.552	1.	1.
667	1	4	1	3	.740	148.693	13.	11.
668	1	2	-6	4	.742	148.784	1211.	945.
669	1	3	0	-7	.755	149.549	15.	17.
670	1	4	-1	-6	.760	149.797	12.	12.
671	1	5	-1	0	.761	149.856	189.	188.
672	1	5	-2	-3	.762	149.905	0.	0.
673	1	1	-6	5	.768	150.214	17.	16.
674	1	2	4	5	.768	150.241	80.	73.
675	1	4	5	-4	.770	150.342	2.	2.
676	1	5	1	0	.770	150.353	187.	174.
677	1	2	8	1	.775	150.575	14.	13.
678	1	0	9	-1	.776	150.644	1.	1.
679	1	3	1	-7	.779	150.772	381.	371.
680	1	4	-5	1	.788	151.234	4.	4.
681	1	4	4	-5	.791	151.358	30.	26.
682	1	0	2	7	.792	151.398	58.	49.
683	1	3	-7	1	.792	151.439	148.	126.
684	1	4	-4	2	.800	151.788	227.	198.
685	1	2	8	-3	.803	151.944	348.	340.
686	1	3	-4	-6	.804	151.984	15.	15.
687	1	5	0	-4	.808	152.143	3.	3.
688	1	3	-4	4	.821	152.728	18.	31.
689	1	1	-8	3	.829	153.038	13.	20.
690	1	1	-3	-7	.829	153.042	75.	120.
691	1	2	-5	-6	.833	153.216	12.	18.
692	1	1	7	-5	.837	153.384	159.	222.
693	1	3	-1	-7	.847	153.793	359.	418.
694	1	3	-7	-3	.854	154.045	57.	63.
695	1	4	-2	3	.858	154.212	366.	396.
696	1	5	1	-4	.862	154.344	42.	46.
DERIVED BRAGG R-FACTOR=					6.58			

values that the models with both iH atoms similarly oriented can be rejected. It is also clear that the *R* values are little affected by the refinement of the site occupancies, rather than their retention at stoichiometric values, for the models in which the orientations differ. But the *R*-value results for the perfect two-fold statistical disorder in the iH orientations (all A and B sites fixed at 0.5) are disquietingly close to those for the ordered, differing orientations models. Since these *R* values differ only by a very small amount in the third digit, they do not give confidence in the choice of the ordered over the disordered model. Instead, confidence comes from the fact that, with two data sets, two programs, and two computers, RRs started with the disordered model consistently produce an ordered model with satisfactorily small e.s.d. One wonders, then, just what is the small systematic aspect of the intensity data that leads to this consistent programmatic choice of the ordered model, and how small is it?

(e) *Basis of the Consistency of the Programmatic Choice*

The central part of the question is that of what Bragg intensity differences accompany the ordered versus disordered models? In both models considered, the

two halves of the cell are constrained to be identical except for the occupancies of the iH sites in the ordered models. The positions of the iH atoms may be written as

H(1A)	H(1B)	H(5A)	H(5B)
x_A	x_B	$x_B + \frac{1}{2}$	$x_A + \frac{1}{2}$
y_A	y_B	$y_B + \frac{1}{2}$	$y_A + \frac{1}{2}$
z_A	z_B	z_B	z_A

The structure factor may then be written as

$$F = F_{iH} + F_{rest},$$

where F_{iH} is the contribution from the inner-hydroxyl hydrogen atoms, the only part that differs with the selection of model, and is given by

$$\begin{aligned} F_{iH} &= f_{1A} \exp[2\pi i\{hx_A + ky_A + lz_A\}] + f_{5B} \exp[2\pi i\{h(x_A + \frac{1}{2}) + k(y_A + \frac{1}{2}) + lz_A\}] \\ &+ f_{1B} \exp[2\pi i\{hx_B + ky_B + lz_B\}] + f_{5A} \exp[2\pi i\{h(x_B + \frac{1}{2}) + k(y_B + \frac{1}{2}) + lz_B\}] \\ &= \exp\{2\pi i(hx_A + ky_A + lz_A)\} [f_{1A} + f_{5B} \exp\{\pi(h+k)\}] \\ &+ \exp\{2\pi i(hx_B + ky_B + lz_B)\} [f_{1B} + f_{5A} \exp\{\pi(h+k)\}]. \end{aligned}$$

With all four iH site occupancies set at 0.5 we have $f_{1A} = f_{1B} = f_{5A} = f_{5B} = 0.5b$, where b is the normal H scattering length. For iH site occupancies 0, 1, 0, 1 (written in the order of Table 4), we have $f_{1A} = f_{5A} = 0$ and $f_{1B} = f_{5B} = b$. For site occupancies 1, 0, 1, 0, we have $f_{1A} = f_{5A} = b$ and $f_{1B} = f_{5B} = 0$. Thus, for $h+k$ even, all three models give identical F values.

For $h+k$ odd, F_{rest} is identically zero. For the disordered (0.5, 0.5, 0.5, 0.5) model, F_{iH} is also identically zero. For the 0, 1, 0, 1 model, for example, F_{iH} is not zero (though it is small), but

$$F_{iH} = b[\exp\{2\pi i(hx_B + ky_B + lz_B)\} - \exp\{2\pi i(hx_A + ky_A + lz_A)\}]$$

which, since there is also the constraint that $x_A = x_B$ and $y_A = y_B$, can be written as

$$F_{iH} = b \exp\{2\pi i(hx_A + ky_A)\} \{\exp(2\pi i lz_B) - \exp(2\pi i lz_A)\}.$$

For the 1, 0, 1, 0 model, F_{iH} is the negative of that for the 0, 1, 0, 1 model, so the intensity is the same. Thus, for $h+k$ odd, the structure factor misses being identically zero only by the small difference in z between the two iH sites at the first x, y .

The calculated and 'observed' Bragg intensities are shown in Table 5 for (a) the first 60 and (b) the last 36 reflections for the 0, 1, 0, 1 model treated in RR CP with the PKA086A data set. Among the first 60, the strongest calculated ($h+k$)-odd reflection is the $01\bar{3}$ with intensity 13 and there are 11 others with intensities >4 . There are six reflections in this set of 60 with calculated intensities more than 100 times larger than that for $01\bar{3}$. In the higher angle set (the last 36), the ($h+k$)-odd intensities tend to be slightly larger (the largest calculated is 18 and 'observed' is 31), while the ($h+k$)-even intensities are generally smaller than in the first set, so that influence of the nonzero ($h+k$)-odd intensities on the course of the RR is a little

more important but, certainly, still very small on the R -values obtained. However, small though they are, the intensities of more than half the $(h+k)$ -odd reflections are numerically nonzero, both calculated and 'observed'. One must conclude that it is, then, these small nonzero intensity values for $h+k$ odd that caused the RRs starting with the perfectly two-fold disordered model for the iH to converge persistently to the ordered model, even though the accompanying reduction in R_{wp} is marginal, in the third digit. Even though, by reason of both small size and overlap, one could not expect to distinguish these reflections visually in the powder diffraction pattern as one can in a single crystal pattern, the operation of the computer program on the pattern as a whole reveals a better statistical correlation with one model (ordered) than the other (disordered) and, therefore, the consistent choice of one model over the other.

Finally, then, it is understood how, even given a starting chance in favour of the perfectly disordered model, the RRs consistently lead to the ordered one-up one-down model, even though the difference in R values would seem to be too small to be significant.

(f) Other Work

When final refinements were carried out (Young and Hewat 1988) in space group $P1$ with the iH occupancies fixed at 0, 1, 0, 1 and 116 parameters refined simultaneously, R_{wp} dropped to 2.03% and R_B to 4.90%. In the end, it was found that the difference in inner-hydroxyl ion orientations is, still, the greatest departure from C-centred symmetry but that all four hydrogen atom 'pairs' also differed from C symmetry, in the x, y plane, by five or more standard deviations.

3. Conclusions

The principal conclusion to be drawn from these two examples is that at least in some cases the Rietveld method can be far more powerful, able to reveal subtle structural details, than one might expect *a priori*.

Acknowledgments

We thank A. W. Hewat very much for collection of the all-important data, for the first RRs with the VAX computer at ILL, and for his considerable intellectual input to the resolution of the kaolinite problem. We also thank B. G. DeBoer for letting us use material that is background to a forthcoming joint paper and for providing constant intellectual stimulus to the resolution of the question posed here about the ability of RR to locate such a small amount of Sb in fluorapatite. We thank A. Sakthivel for assistance with computer-handling and for helpful discussions of both problems.

References

- Adams, J. M. (1983). *Clays Clay Miner.* **31**, 352-6.
- DeBoer, B. G., Sakthivel, A., Cagle, J. R., and Young, R. A. (1988). Determination of the antimony substitution site in calcium fluorapatite from powder X-ray diffraction data.
- Hewat, A. W. (1973). The Rietveld computer program for refinement of neutron powder diffraction patterns modified for anisotropic thermal vibration. Harwell Rep. No. AERE-R7350.

- Rietveld, H. M. (1969). *J. Appl. Crystallogr.* **2**, 65-71.
- Sudarsanan, K., Mackie, P. E., and Young, R. A. (1972). *Mater. Res. Bull.* **7**, 1331-8.
- Suitch, P. R., and Young, R. A. (1983). *Clays Clay Miner.* **31**, S17-32.
- Thompson, J. G. (1984). *Clays Clay Miner.* **35**, 233-4.
- Thompson, J. G., and Withers, R. L. (1987). *Clays Clay Miner.* **35**, 237-9.
- Wiles, D. B., and Young, R. A. (1981). *J. Appl. Crystallogr.* **14**, 149-51.
- Young, R. A., and Hewat, A. W. (1988). Verification of the triclinic crystal structure of kaolinite. *Clays Clay Miner.* (in press).
- Young, R. A., Sakthivel, A., and DeBoer, B. G. (1988). X-ray Rietveld structure refinements of Ca, Sr, and Ba meta-antimonates.

Manuscript received 21 August, accepted 11 November 1987